

5-11-2019

# Investigation of the Catalytic Properties of Cerium(IV) Oxide in Metal Oxide Laser Ionization-Mass Spectrometry

Madison McMinn  
madison.mcminn@siu.edu

Follow this and additional works at: [https://opensiuc.lib.siu.edu/uhp\\_theses](https://opensiuc.lib.siu.edu/uhp_theses)

---

## Recommended Citation

McMinn, Madison, "Investigation of the Catalytic Properties of Cerium(IV) Oxide in Metal Oxide Laser Ionization-Mass Spectrometry" (2019). *Honors Theses*. 457.  
[https://opensiuc.lib.siu.edu/uhp\\_theses/457](https://opensiuc.lib.siu.edu/uhp_theses/457)

This Dissertation/Thesis is brought to you for free and open access by the University Honors Program at OpenSIUC. It has been accepted for inclusion in Honors Theses by an authorized administrator of OpenSIUC. For more information, please contact [opensiuc@lib.siu.edu](mailto:opensiuc@lib.siu.edu).

**Investigation of the Catalytic Properties of Cerium(IV) Oxide in  
Metal Oxide Laser Ionization-Mass Spectrometry**

Madison H. McMinn

A thesis submitted to the University Honors Program &  
Department of Chemistry and Biochemistry in partial fulfillment  
of the requirements for the Honors Diploma with Thesis,  
Chemistry Honors, and American Chemical Society Certification

Department of Chemistry and Biochemistry

Southern Illinois University Carbondale

May 2019

## **Abstract**

Matrix-assisted laser desorption/ionization-mass spectrometry (MALDI-MS) has emerged in recent years as one of the most powerful tools available for characterizing the molecules involved in the biochemistry of life. Metal oxide laser ionization (MOLI) is a recently described variation on MALDI in which a metal oxide, rather than an organic acid, is utilized as the matrix. Unlike other metal oxides, Cerium(IV) Oxide ( $\text{CeO}_2$ ) demonstrates a unique property of laser induced catalytic side chain cleavage of fatty acids when applied to phospholipids and energized by standard lasers found in MALDI-TOF-MS instruments.

In previous work, a technique for  $\text{CeO}_2$  deposition on mouse brain tissue was developed that allows fatty acyl catalysis directly from tissue for possible bacterial identification. Although MOLI using  $\text{CeO}_2$  was shown to be promising for this application, the mechanism of fatty acyl catalysis remains poorly understood. In the current studies, a negative ion mode calibration mixture is first optimized to ensure mass-to-charge ( $m/z$ ) assignments are accurate thereby allowing structural assignments to be confirmed. This calibrant mixture is then used in the analysis of a phospholipid standard used in previous work; palmitoyl-2-oleoyl-glycero-3-phosphocholine (POPC). This work ensures that the mouse brain imaging results obtained earlier can be replicated on the Bruker MicroFlex MALDI-TOF-MS. With this assurance, structural variants of POPC are studied to determine how slight variations in structure affect the catalytic cleavage with a goal to gain insight into the cleavage mechanism. Additionally, computational studies are performed to gain insight into the structural and electronic properties of phospholipids and their derivatives.

### **Acknowledgments**

I would like to thank Dr. Gary Kinsel and Dr. Mary Kinsel for their support in this undergraduate research experience, and in many aspects of my undergraduate career. Without their help, I am doubtful I would have been able to achieve as much as I have during my time at SIUC. Their support in and out of the classroom and research lab is unparalleled.

I would also like to thank Chelsea Bridgmohan-Gemeinhardt and Dr. Lichang Wang for help with the computational studies conducted in this thesis, as well as their support throughout my undergraduate studies in chemistry.

I would also like to thank the Office of the Vice Chancellor for Research and the McNair Scholars Program, for providing funding for this project. Especially, Dr. Rhetta Seymour of McNair and Vice Chancellor of Research Dr. Jim Garvey for their support throughout this project and many others during my time at SIUC.

I am forever grateful to the SIUC Honors Program for their guidance and support, especially my mentors Brenda Sanders and Elizabeth Donoghue, along with the entire Honors office.

I would also like to thank Dr. Nathalie Agar, as my work in her lab last summer at Harvard was the inspiration behind this project.

Finally, I would like to thank my friends and family for their support and encouragement over these last four years.

**Table of Contents**

<u>Section</u>	<u>Page</u>
<i>Abstract</i> .....	1
<i>Acknowledgements</i> .....	2
<i>Table of Contents</i> .....	3
<i>List of Figures</i> .....	4
<i>List of Tables</i> .....	5
<i>CHAPTER 1 – Introduction</i> .....	6 -11
<i>CHAPTER 2 – Materials and Methods</i> .....	12 - 13
<i>CHAPTER 3 – Results and Discussion</i> .....	14 – 19
<i>Experimental Studies</i> .....	14-15
<i>Computational Studies</i> .....	16-19
<i>Conclusion &amp; Future Directions</i> .....	20
<i>References</i> .....	21-22

## List of Figures & Tables

<u>Figure</u>	<u>Page</u>
<i>Figure 1</i> Mass spectra of lipid standards with respective molecular structures. <sup>6</sup> .....	8
<i>Figure 2</i> MOLI MSI of control mouse brain tissue. Coronal sections (12 $\mu\text{m}$ thickness) of frozen mouse spotted with a solution of $\text{CeO}_2$ in isopropanol, acquired using 100 $\mu\text{m}$ pixel resolution. <sup>6</sup> .....	9
<i>Figure 3</i> Labeled <i>sn</i> -1 and <i>sn</i> -2 positions on the glycerol backbone.....	11
<i>Figure 4</i> Mass spectra of phospholipid standards HOPC, OPPC, POPC, and calibration mixture in negative ion mode.....	14
<i>Figure 5</i> Lipid structure of A) HOPC B) OPPC and C) POPC	15
<i>Figure 6</i> Gaussian generated optimized structures of phospholipids and their Mulliken charges for A) POPC, B) POPS, C)HOPC, and D) POPE .....	18

**List of Tables**

<u>Table</u>	<u>Page</u>
<i>Table 1.</i> Bond distance and bond angle values for phospholipids from computational studies.....	<i>16</i>
<i>Table 2</i> Mulliken charges for phospholipids from computational studies.....	<i>17</i>

## **Chapter 1 : Introduction**

Matrix-Assisted Laser Desorption/Ionization Mass Spectrometry (MALDI-MS) has emerged in recent years as one of the most powerful tools available for characterizing the molecules involved in the biochemistry of life. In recent years, MALDI-MS has been found to be a valuable tool in a number of different fields such as molecular biology, biotechnology, and biomedicine.<sup>1-5</sup> MALDI coupled with Mass Spectrometry Imaging (MSI) is an emerging and powerful analytical technique which allows the spatially resolved characterization of a wide range of analytes within biological specimens.<sup>6</sup> In contrast to commonly used imaging techniques, such as immunohistochemistry (IHC), MALDI-MSI allows for the untargeted analysis of tissue sections.<sup>7</sup> Although many of the original applications of MALDI-MSI focused on protein analyses,<sup>8</sup> there has been significant progress in utilization of this technique to characterize drugs<sup>9-11</sup> and lipids<sup>12</sup> in tissue specimens.

Metal oxide laser ionization (MOLI) is a recently described variation on MALDI in which a metal oxide, rather than an organic acid, is utilized as the matrix.<sup>13</sup> Like MALDI, MOLI utilizes laser energy to generate ions that are measured by a mass spectrometer, most commonly a time of flight (TOF) mass spectrometer. Compared with MALDI, one of the central advantages of MOLI is the absence of matrix ion peaks, which can obscure ions from the biological specimen in the small molecule range ( $m/z < 1000$ ). Most commonly, when MOLI MS is used, analyte ionization of lipids occurs by protonation, or sodiation, due to interactions with the Lewis acid/base sites on the metal oxide. However, as studies have continued, it has been found that the ionization mechanism can vary between metal oxides.<sup>14</sup>

For certain metal oxides, such as nickel (II) oxide (NiO), the method of ionization is thought to involve Lewis acid/base interactions between the cation/anion pairs of the metal oxide



and the analyte, resulting in the protonation from one surface-bound analyte to another without involving solvent or surface-absorbed water.<sup>15</sup> For others, such as calcium oxide (CaO), analyte ionization occurs due to interactions with Lewis acid/base sites on the metal oxide, and results in a calcium adduct of a fatty acid carboxylate.<sup>16</sup> More recently, cerium(IV) oxide (CeO<sub>2</sub>), a rare earth lanthanide, has also been utilized in MOLI-MS. However, unlike the other metal oxides, CeO<sub>2</sub> demonstrates a unique property of laser induced catalysis of fatty acyl cleavage when applied to phospholipids and energized by standard lasers found in commonly used and commercially-available MALDI-TOF-MS instruments, as seen in Figure 1.<sup>15</sup> Furthermore, instead of forming a protonated or sodiated ion, as observed with the other metal oxides, CeO<sub>2</sub> generates negative ions exclusively.<sup>14,16,18,19,20</sup>

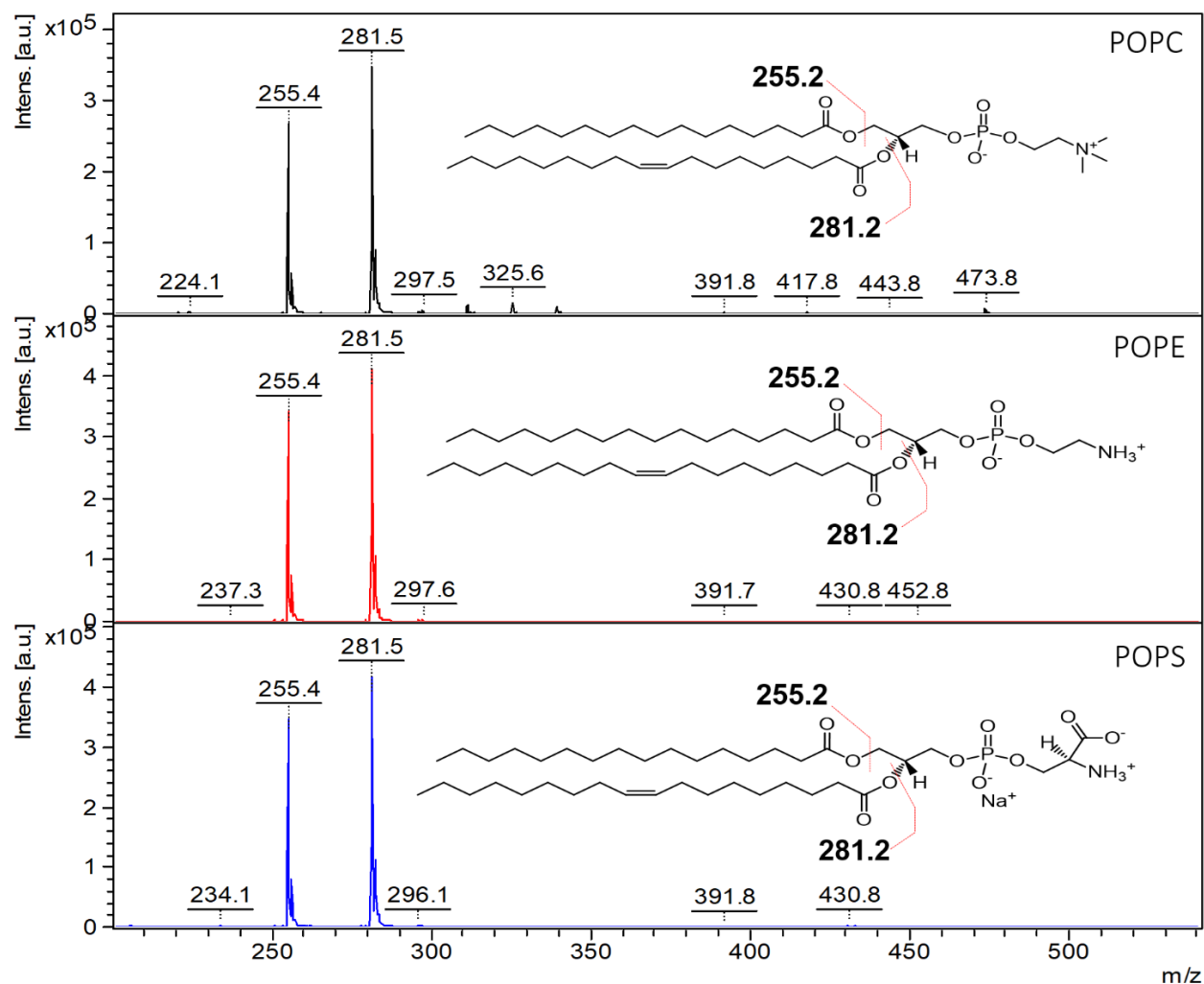


**Figure 1.** Mass spectra of lipid standards with respective molecular structures.<sup>19</sup>

This property of laser-induced catalytic cleavage by  $\text{CeO}_2$  provides a unique opportunity in various biological and clinical applications in which fatty acid profiling may be needed.<sup>15,16</sup> Beyond clinical applications,  $\text{CeO}_2$ -based materials also have a variety of applications as a catalytic system in fuel cells, for thermochemical water-splitting, in various organic reactions, and for photocatalysis.<sup>17</sup> Because of this involvement of  $\text{CeO}_2$  in a variety of fields, and the potential it has to impact future technologies, further investigations of the biological catalysis properties of this compound are warranted.

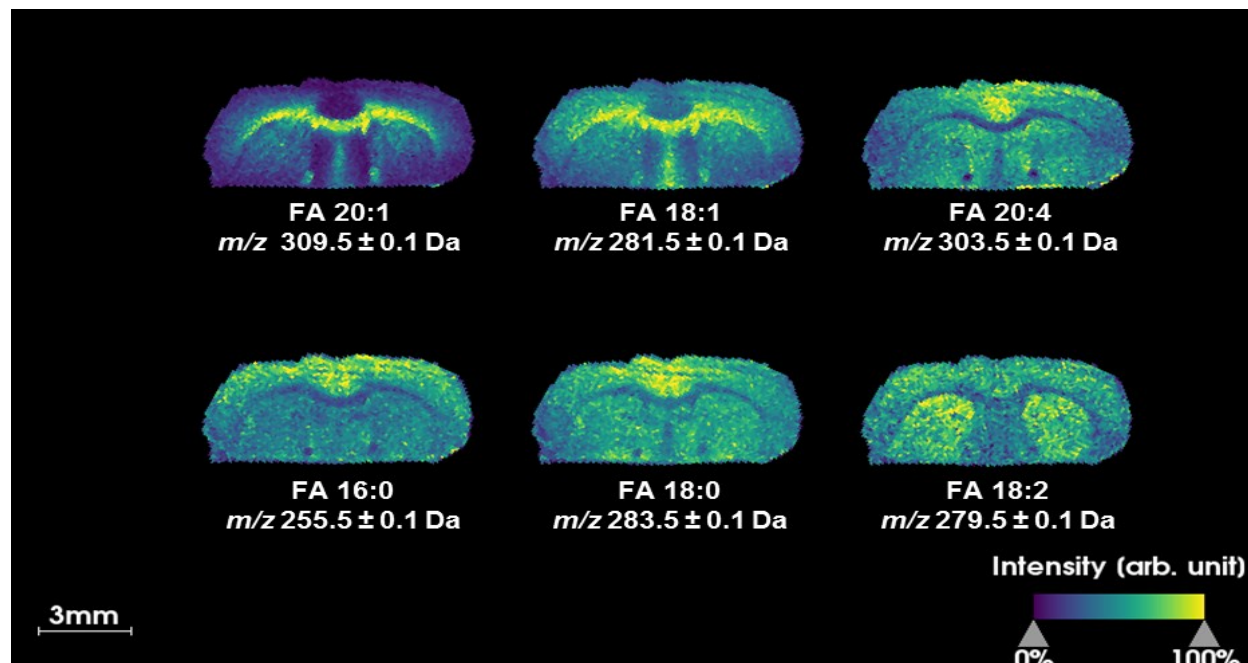


**Figure 2.** MOLI MSI of control mouse brain tissue. Coronal sections (12  $\mu\text{m}$  thickness) of frozen mouse spotted with a solution of  $\text{CeO}_2$  in isopropanol, acquired using 100  $\mu\text{m}$  pixel resolution.<sup>19</sup>

Until recently, however, MOLI with  $\text{CeO}_2$  had not been used in conjunction with MALDI-MSI. This oversight was addressed during summer 2018 through studies performed at the Harvard Medical School in the Agar group. In these studies a method was developed and optimized for  $\text{CeO}_2$  deposition on biological tissue for subsequent MOLI-MSI characterization with direct on-tissue fatty acyl catalysis. An example of the results of these investigations is shown in Figure 2 and further details are included in a manuscript recently accepted for publication.<sup>19</sup>

Although MOLI-MSI using  $\text{CeO}_2$  shows considerable promise, the mechanism of fatty acyl catalysis is still unknown. As stated above, with other metal oxides analyte ionization of phospholipids typically occurs by protonation, or sodiation, due to interactions with the Lewis

acid/base sites on the metal oxide. However, neither protonated or sodiated lipid fragments are present with CeO<sub>2</sub>-induced catalysis, indicating that the mechanism of cleavage is unique. It is postulated that much of the catalytic activity of CeO<sub>2</sub> arises from oxygen vacancy defects in the surface which occur at MALDI-like conditions (high temperature, low pressure).<sup>20</sup>

Furthermore, previous research in the use of CeO<sub>2</sub> as a matrix for MOLI-MS, focused on bacterial lipid extracts for strain-level identification. As a result, individual phospholipids were not analyzed, and only complex mixtures derived from bacteria were characterized. From these studies, bacteria were identified based on the mass spectral fingerprint generated for each strain of bacteria studied.<sup>18,20</sup> In order to aid in the understanding of the catalytic properties of CeO<sub>2</sub>, single phospholipids must be analyzed in order to study the impact of small structural differences not yet observed with CeO<sub>2</sub> MOLI-MS.

Previous studies of individual phospholipids have been performed by conventional MALDI-MS which give some insight into the ions that are formed from these compounds and their relevance to compound identification. Specifically, in order to fully identify a phospholipid, the fatty acyl chain located at each position on the glycerol backbone must be identified. In the typical two-chain phospholipid, these positions are identified as the *sn*-1 and *sn*-2 positions, as shown in figure 3.<sup>21</sup> In positive ion MALDI-MS studies using 2,5-dihydroxybenzoic acid (DHB) as the matrix phospholipids will form two main adducts resulting from proton attachment and lithium attachment. Experimental results show that selective loss of the fatty acyl chain occurs at the *sn*-2 position for protonated ions, while loss at the *sn*-1 position occurs for lithium adducts.<sup>21</sup> Since there is a differentiation in adduct formation depending on the adduct formed, it is important to note if the *sn*-1 or *sn*-2 has any effect on catalysis of the fatty acyl chains when CeO<sub>2</sub> is utilized.

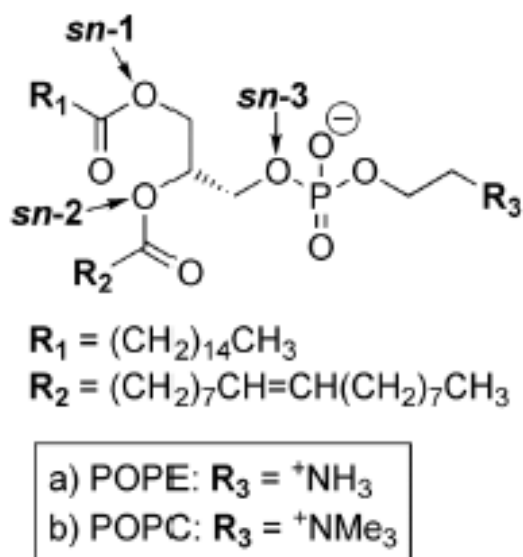


**Figure 3.** Labeled *sn*-1 and *sn*-2 positions on the glycerol backbone<sup>21</sup>

In the present research, experimental and computational studies are performed to answer a number of questions about the catalytic nature of  $\text{CeO}_2$ . First, experimental studies are performed to determine if the orientation of the phospholipid, as well as the functional group connecting the fatty acid chain, affects cleavage. In addition, computational studies are performed to confirm that the head group, as well as the orientation of the phospholipid, has no impact on the efficiency of cleavage of the fatty acid chains. This is done by examining the Mulliken charges, bond angles, and bond lengths.

## **Chapter 2: Materials and Methods**

### **Materials**

1-palmitoyl-2-oleoyl-glycero-3-phosphocholine (POPC), 1-O-hexadecyl-2-oleoyl-sn-glycerol-3-phosphocholine (HOPC), 1-oleoyl-2-palmitoyl-sn-glycero-3-phosphocholine (OPPC) were obtained from Avanti Polar Lipids (Alabaster, AL). Cerium (IV) oxide ( $\text{CeO}_2$ ) (<5  $\mu\text{m}$ , 99.9% purity), L-ascorbic acid (99% purity), sinapic acid (99%), methanol (MeOH), and chloroform ( $\text{CHCl}_3$ ) were purchased from Sigma-Aldrich (St. Louis, MO, USA). L-glutamic acid was purchased from Aldrich Chem. Co. (Milwaukee, WI).

### **Methods**

#### *Creation of Calibration Mixture*

A calibration mixture was prepared for negative ion mode using a 9:1 ratio of matrix:analyte. The matrix used was sinapic acid; prepared at a concentration of 10 mM in methanol. The analyte was a 1:1 glutamic:ascorbic acid mixture. Glutamic and ascorbic acid were prepared at a concentration of 10 mM in DI water. For analysis, 0.5  $\mu\text{L}$  was deposited on the stainless steel MALDI target. Mass spectra of these prepared MALDI samples were then obtained using a commercial Bruker Microflex time-of-flight mass spectrometer operating at 337nm. The instrument was operated in linear, negative ion mode and the detector used is a microchannel plate detector; where the detection range was set from 20 to 1900 m/z.

#### *Analysis of Phospholipid Standards*

Phospholipid standards were prepared at concentrations of 0.329 M in a 2:1 (v/v) solution of chloroform:methanol and stored at -20 C. Cerium(IV) Oxide was prepared by suspending 100

mg of CeO<sub>2</sub> in 1 mL of isopropanol. For analysis by MALDI-MS, 0.5 μL of CeO<sub>2</sub> was deposited on the stainless steel MALDI target plate and allowed to dry. Next, 0.5 μL of the lipid standard was deposited directly on top of the CeO<sub>2</sub>. Mass Spectra was collected under the same conditions as the calibration mixture.

### *Computational Studies*

The *Gaussian 16* Density Functional Theory (DFT) package was utilized for computational studies with B3LYP functionals and the 6-31g+(d,p) basis set. A solvent model CPCM (implicit model) was included using chloroform as the solvent. Computational studies were used to find the bond length, bond angle, and the Mulliken charges around the suspected cleavage site. The Mulliken charge is the partial atomic charge attributed to a particular atom within a molecule.

### Chapter 3: Results and Discussion

#### Experimental Studies

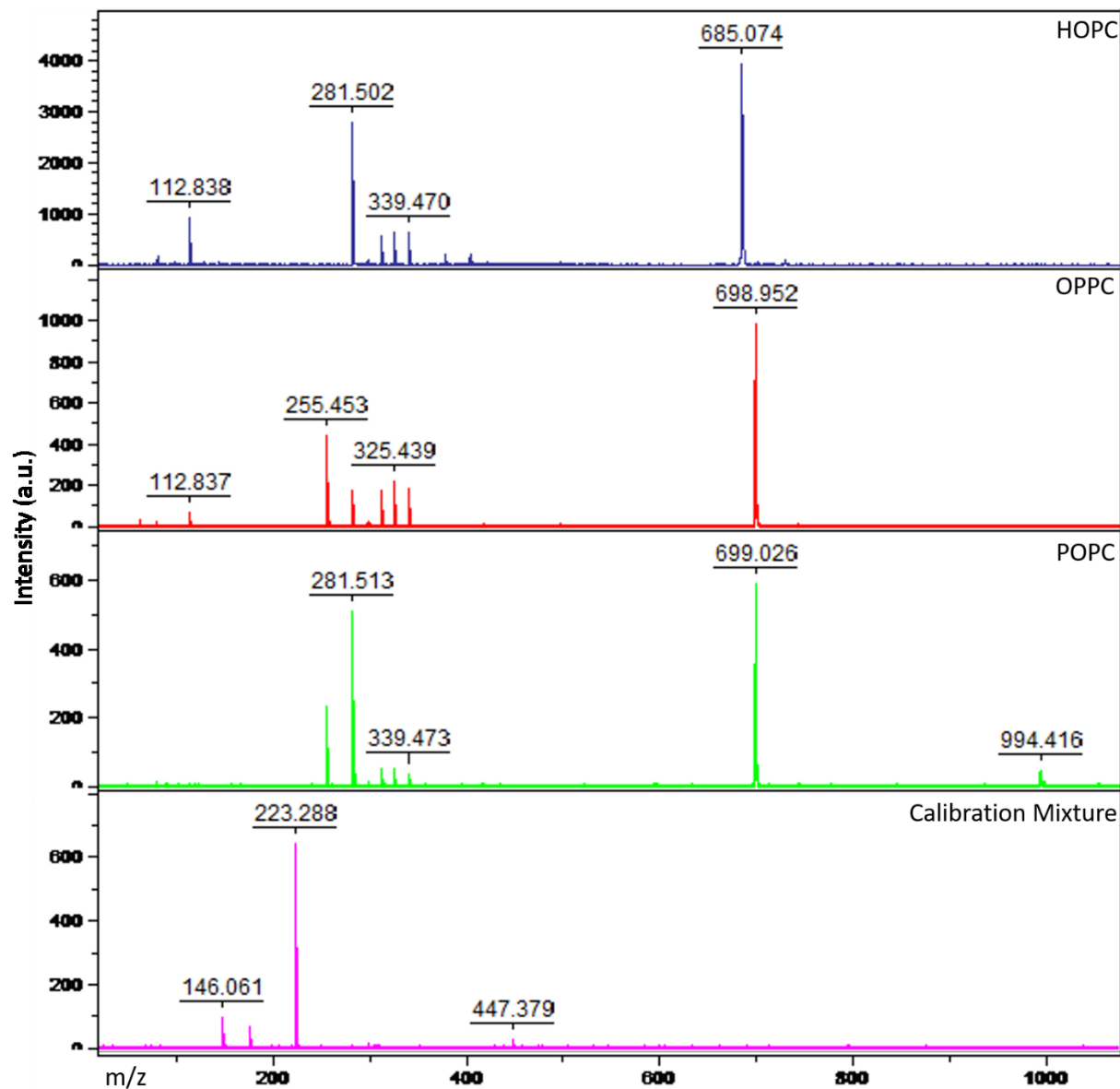


**Figure 4.** Mass spectra of phospholipid standards HOPC, OPPC, POPC, and calibration mixture in negative ion mode



Figure 4 shows representative mass spectra of the three different phospholipid standards tested in this experiment. The phospholipid standards tested were variants on POPC. In POPC, the C16:0 fatty acid chain is present in the *sn*-1 position and the C18:1 Chain is in the *sn*-2 position. For OPPC, this order is reversed, as seen in figure 5. From the spectra collected, it appears that cleavage of the *sn*-2 position is favored. As a result, C18:1 is cleaved with more efficiency than C16:0 for POPC but the situation is reversed for OPPC.

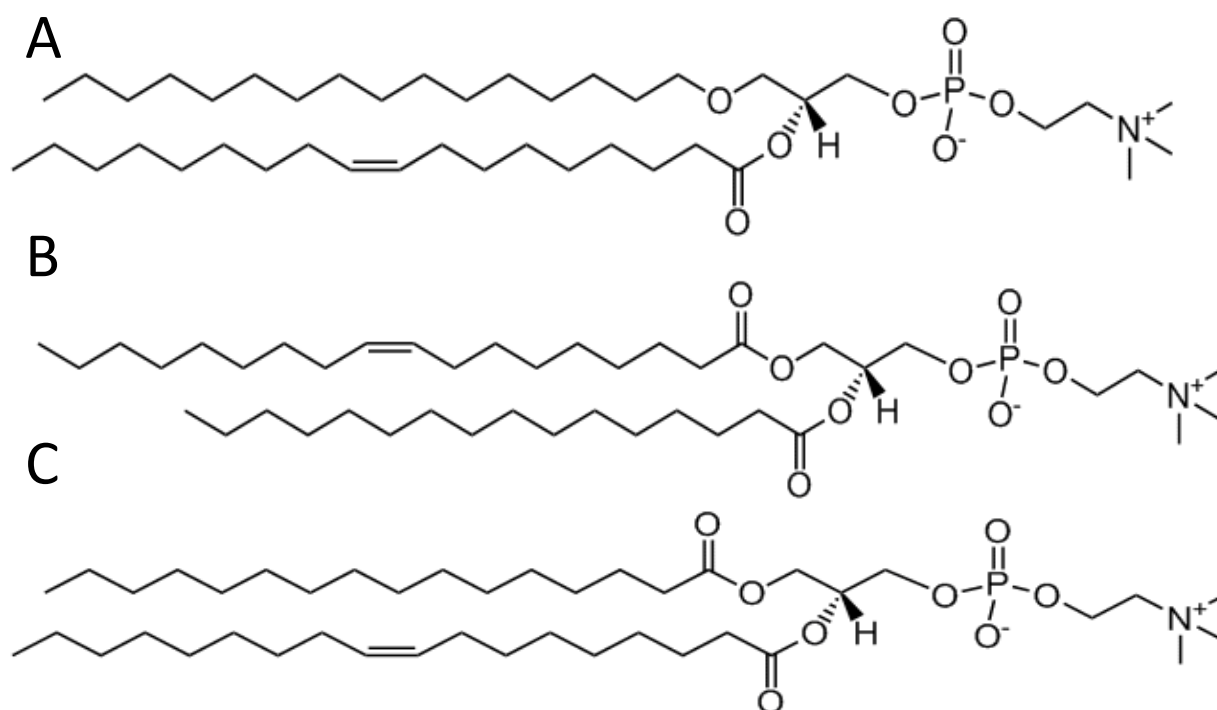


**Figure 5. Lipid structure of A) HOPC and B) OPPC C) POPC**

The efficiency of cleavage of the fatty acid chains is affected even more by a change in the functional group connecting the fatty acid chain to the phospholipid head. In HOPC, the functional group connecting the C16:0 chain is changed from a carboxyl group to an ether group. From the resulting mass spectrum of HOPC, it is seen that when the functional group is changed, no cleavage occurs. The expected fragment, if cleavage occurred at the oxygen, would be

242.261 m/z. However, this is not present in the mass spectrum, suggesting no fragment is formed from the ether functional group.

### *Computational Studies*

**Table 1.** Bond distance and bond angle values for phospholipids from computational studies.

HOPC		POPC		POPS		POPE	
atoms	bond distance (Å)	atoms	bond distance (Å)	atoms	bond distance (Å)	atoms	bond distance (Å)
1-2	1.52595	1-2	1.44566	1-2	1.44311	1-2	1.44566
2-3	1.41996	2-3	1.35147	2-3	1.35393	2-3	1.35147
4-5	1.4534725	4-5	1.45552	4-5	1.45158	4-5	1.45552
5-6	1.34725	5-6	1.35026	5-6	1.35443	5-6	1.35026
atoms	angle (°)	atoms	angle (°)	atoms	angle (°)	atoms	angle (°)
1-2-3	108.83686	1-2-3	116.66947	1-2-3	116.5455	1-2-3	116.66947
4-5-6	121.87937	4-5-6	121.62714	4-5-6	121.34574	4-5-6	121.62714

**Table 2.** Mulliken charges for phospholipids from computational studies.

HOPC		POPC		POPS		POPE	
atom	mulliken charge (au)	atom	mulliken charge (au)	atom	mulliken charge(au)	atom	mulliken charge(au)
1	-0.359	1	-0.413	1	-0.101	1	-0.419
2	-0.306	2	-0.305	2	-0.708	2	-0.357
3	0.535	3	0.529	3	0.905	3	0.045
4	0.420	4	0.422	4	0.025	4	0.608
4	-0.187	4	-0.188	4	-0.701	4	-0.200
5	-0.117	5	-0.085	5	0.930	5	-0.068
6	-0.359	6	-0.413	6	-0.101	6	-0.419

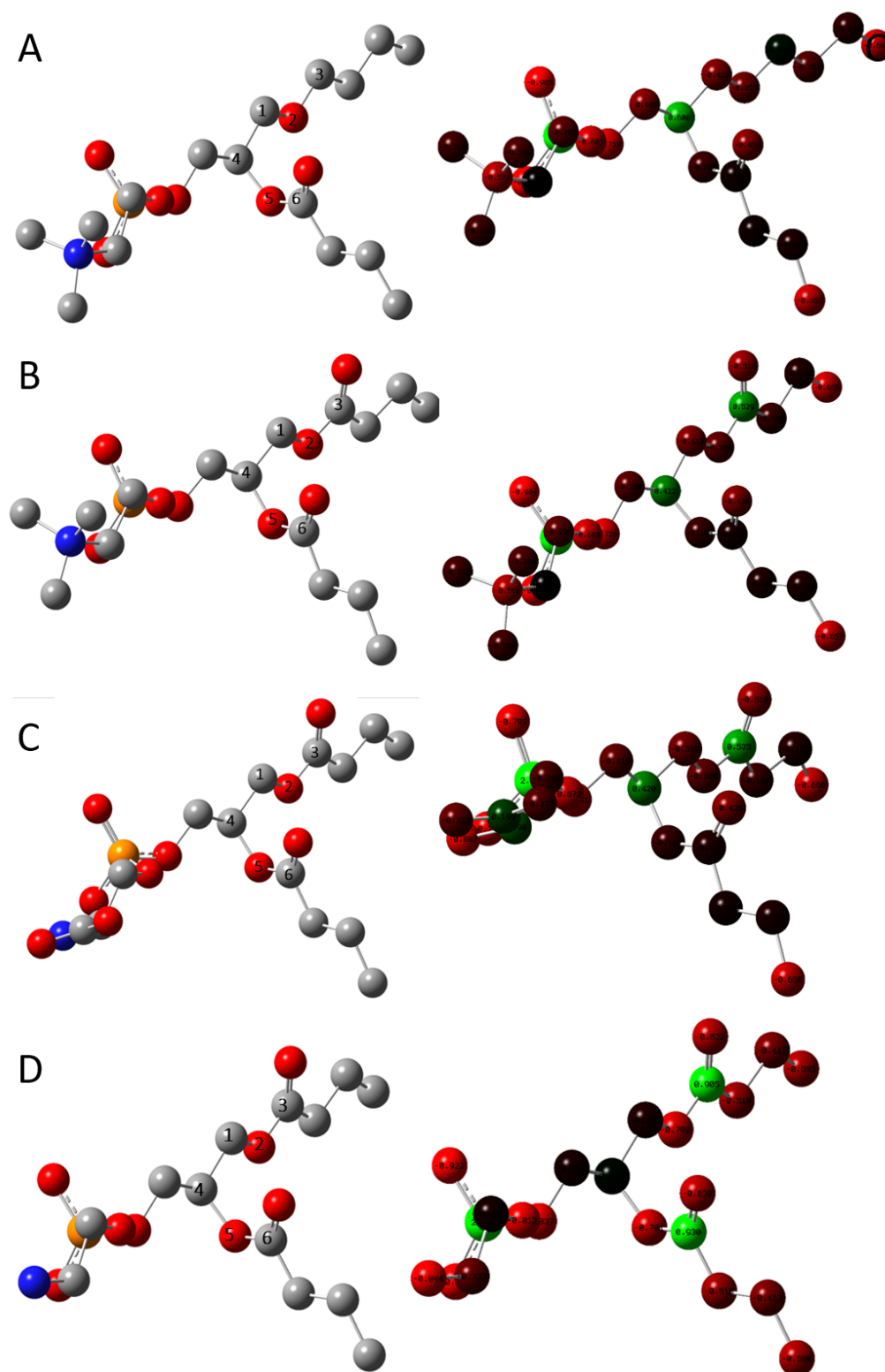


**Figure 6.** *Gaussian* generated optimized structures of phospholipids and their Mulliken charges for A) POPC, B) POPS, C)HOPC, and D) POPE

For the computational studies, the bond distance, angle, and Mulliken charges were compared for the four phospholipids tested. Calculations were performed using a truncated fatty acid chain, because no cleavage was observed to occur in that region. When comparing molecules of different head groups, little variation in the bond distances and bond angles occurred (figure 5, table 1). However, in HOPC, when the functional group is changed from a carboxyl to an ether, the geometry of the lipid is greatly affected. There is an increase in bond distance between atoms 2 and 3, which is the location of expected cleavage. Also, the bond angle of the ether group is much smaller than that of the corresponding carboxyl group in POPC. These differences may impact why cleavage does not occur experimentally at this site.

Mulliken charges are way to study the charges on individual atoms in a molecule. Atoms with a larger charge difference are expected to have a stronger bond, based on Coulomb's law. From the computational studies performed, for POPC, POPS, and HOPC, there is a larger charge difference in the *sn*-2 position than in the *sn*-1 position. This would suggest that cleavage of the *sn*-1 position would be favored over the *sn*-2. However, this is not observed experimentally. Further computational studies need to be performed to investigate these phenomena.

### **Conclusion & Future Directions**

In this study, we demonstrate, for the first time, the use of MOLI-MS to discriminate between phospholipids with the same fatty acid side chains, but varied functional groups or spatial orientation. Future studies need to be done experimentally and computationally to further elucidate the cleavage mechanism of CeO<sub>2</sub>. Computationally, studies need to be completed to calculate the bond energy at the sites of expected cleavage. This will give more accurate information than the Mulliken charges. Additionally, modeling the CeO<sub>2</sub> surface and allowing the phospholipids to interact with the surface to which energy is applied will better simulate MALDI conditions than the current calculations. Experimentally, more standards need to be tested in order to examine how more differences in structure affects cleavage. This would include lipids with different head groups, different functional group modifications, and different fatty acid chains.

### References

1. Dreisewerd, Klaus *Anal. Bioanal. Chem.* **2014**, 406(1), 2261-2278.
2. Bucknall, M. et al. *J. Am. Soc. Mass Spectrom.* **2002**, 13(1), 1015-1027.
3. Schiller, J. et al. *Prog. Lipid Res.* **2004**, 43(1), 449-488.
4. Jurinke, C. et al *Mol. Biotechnol.* **2004**, 26(2), 147-164.
5. Kaufmann, R. *J. Biotechnol.* **1995**, 41(1), 155-175
6. Reyzer M.L., Caprioli R.M. *J Proteome Res.* **2005**, 4(4), 1138-1142.
7. Schwamborn K, Caprioli R.M *Nat Rev Cancer.* **2010**, 10(1), 639-646.
8. Caprioli, R.M.; Farmer, T.B.; Gile, J. *Anal. Chem.* **1997**, 69(23), 4751-4760.
9. Stoeckli, M.; Farmer, T. B.; Caprioli, R. M. *J. Am. Soc. Mass Spectrom.* **1999**, 10(1), 67-71.
10. Castellino S, Groseclose MR, W. D. *Bioanalysis* **2011**, 3(21).
11. Liu, X. et al. *Sci. Rep.* **2013**, 3, 2859.
12. Gode, D.; Volmer, D. A. *Analyst* **2013**, 138 (5), 1289–1315.
13. Prideaux, B.; Lenaerts, A.; Dartois, V. *Curr. Opin. Chem. Biol.* **2018**, 44, 93–100.
14. Voorhees, K. J.; Saichek, N. R.; Jensen, K. R.; Harrington, P. B.; Cox, C. R. *J. Anal. Appl. Pyrolysis* **2015**, 113, 78–83.
15. Choe, S. S.; Huh, J. Y.; Hwang, I. J.; Kim, J. I.; Kim, J. B. *Front. Endocrinol. (Lausanne)*. **2016**, 7, 30.
16. Voorhees, K. J.; McAlpin, C. R.; Cox, C. R. *J. Anal. Appl. Pyrolysis* **2012**, 98, 201–206.
17. Hodson, L.; Skeaff, C. M.; Fielding, B. A. *Prog. Lipid Res.* **2008**, 47 (5), 348–380.
18. Voorhees, K. J.; Jensen, K. R.; McAlpin, C. R.; Rees, J. C.; Cody, R.; Ubukata, M.; Cox, C. R. *J. Mass Spectrom.* **2013**, 48 (7), 850–855.

19. McMinn MH, Basu SS, Regan MS, Randall EC, Lopez BGC, Clark AR, Cox CR, Agar NYR. Metal Oxide Laser Ionization Mass Spectrometry Imaging (MOLI-MSI) using Cerium (IV) Oxide. *Anal. Chem.* **2019**, Article ASAP.
20. Cox, C. R.; Jensen, K. R.; Saichek, N. R.; Voorhees, K. J. *Sci. Rep.* **2015**, *5*, 10470.
21. Pridmore, D.J. et al. *Analyst* **2011**, *12*(1), 1-7.